

Type I Interferon Responses Drive Intrahepatic T cells to Promote Metabolic Syndrome

Magar Ghazarian^{1,2,*†}, Xavier S. Revelo^{1,*†}, Mark K. Nøhr^{1,*}, Helen Luck^{1,2,*}, Kejing Zeng^{1,3}, Helena Lei^{1,*}, Sue Tsai^{1,*}, Stephanie A. Schroer¹, Yoo Jin Park¹, Melissa Hui Yen Chng⁴, Lei Shen⁵, June Ann D'Angelo⁶, Peter Horton^{7,8}, William C. Chapman⁹, Diane Brockmeier¹⁰, Minna Woo¹, Edgar G. Engleman⁴, Oyedele Adeyi^{11,12}, Naoto Hirano^{2,13}, Tianru Jin¹, Adam J. Gehring^{6,14}, Shawn Winer^{1,12,15,‡,§}, and Daniel A. Winer^{1,2,11,12,*‡,§}

¹Division of Cellular and Molecular Biology, Diabetes Research Group, Toronto General Research Institute, University Health Network, 101 College Street, Toronto, Ontario M5G 1L7, Canada

²Department of Immunology, University of Toronto, 1 King's College Circle, Toronto, Ontario M5S 3B3, Canada

³Department of Endocrinology and Metabolism, Third Affiliated Hospital of Sun Yat-sen University, Guangzhou 510630, China

⁴Department of Pathology, Stanford University School of Medicine, Palo Alto, CA 94205, USA

⁵Shanghai Institute of Immunology, Shanghai Jiao Tong University School of Medicine, Shanghai 200240, China

⁶Department of Molecular Microbiology and Immunology, Saint Louis University School of Medicine, St. Louis, MO 63104, USA

⁷Methodist University Hospital Transplant Institute, Memphis, TN 38104, USA

⁸Division of Abdominal Transplant, Saint Louis University School of Medicine, St. Louis, MO 63104, USA

⁹Division of Abdominal Transplant, Washington University School of Medicine, St. Louis, MO 63110, USA

¹⁰Mid-America Transplant Services, St. Louis, MO 63110, USA

¹¹Department of Pathology, University Health Network, 200 Elizabeth Street, Toronto, Ontario M5G 2C4, Canada

§Corresponding author. shawn.winer@utoronto.ca (S.W.); dan.winer@uhn.ca (D.A.W.).

*Present address: 10-352 Toronto Medical Discovery Tower, Toronto, Ontario M5G 1L7, Canada.

†These authors contributed equally to this work.

‡Co-senior authors.

AUTHOR CONTRIBUTIONS

S.W., D.A.W., and M.G. conceived the study, designed experiments, and wrote the manuscript. M.G. and X.R. designed and performed experiments, interpreted results, generated figures and tables, and wrote the manuscript. H.Luck., K.Z., M.C., L.S., H.Lei, M.K.N., S.S., Y.P., and S.T. performed experiments. A.J.G., J.A.D., P.H., W.C.C., and D.B. performed experiments and provided data from the human cohort from St. Louis University Hospital. O.A., S.W., and D.A.W. analyzed histological sections. M.W., E.E., N.H. and T.J. provided feedback and supervised aspects of the study. S.W. and D.A.W. supervised the overall implementation of the study.

COMPETING INTERESTS

The authors have declared that they have no conflict of interest.

¹²Department of Laboratory Medicine and Pathobiology, University of Toronto, Toronto, Ontario M5S 1A8, Canada

¹³Campbell Family Cancer Research Institute, University Health Network, Toronto, Ontario M5G 2M9, Canada

¹⁴Toronto Centre for Liver Disease, University Health Network, Toronto, Ontario M5G 2C4, Canada

¹⁵Department of Laboratory Medicine, St. Michael's Hospital, Toronto, Ontario M5B 1W8, Canada

Abstract

Obesity-related insulin resistance is driven by low-grade chronic inflammation of metabolic tissues. In the liver, non-alcoholic fatty liver disease (NAFLD) is associated with hepatic insulin resistance and systemic glucose dysregulation. However, the immunological factors supporting these processes are poorly understood. We found that the liver accumulates pathogenic CD8⁺ T cell subsets which control hepatic insulin sensitivity and gluconeogenesis during diet-induced obesity in mice. In a cohort of human patients, CD8⁺ T cells represent a dominant intrahepatic immune cell population which links to glucose dysregulation. Accumulation and activation of these cells are largely supported by type I interferon (IFN-I) responses in the liver. Livers from obese mice upregulate critical interferon regulatory factors (IRFs), interferon stimulatory genes (ISGs), and IFN α protein, while IFN α R1^{-/-} mice, or CD8-specific IFN α R1^{-/-} chimeric mice are protected from disease. IFN α R1 inhibitors improve metabolic parameters in mice, while CD8⁺ T cells and IFN-I responses correlate with NAFLD activity in human patients. Thus, IFN-I responses represent a central immunological axis that governs intrahepatic T cell pathogenicity during metabolic disease.

INTRODUCTION

Obesity is a major risk factor for the development of type 2 diabetes and its precursor, insulin resistance (IR). Multiple factors contribute to obesity-induced IR, but low grade chronic inflammation of metabolic tissues is one central factor in its development (1, 2). This inflammation is driven by both innate and adaptive cells of the immune system. During obesity, T cell composition in various tissues is altered to favor inflammatory subsets that promote IR. In particular, CD4⁺ and CD8⁺ T cells are pivotal in orchestrating visceral adipose tissue (VAT) inflammation and metabolic disease during obesity (3, 4). In addition to VAT, the liver is a key site that becomes altered during obesity (5). Non-alcoholic fatty liver disease (NAFLD), and its progressed inflammatory state, non-alcoholic steatohepatitis (NASH), are manifestations of metabolic syndrome in the liver and have emerged as leading causes of abnormal liver function (6). NAFLD is characterized by increased intrahepatic fat content which is tightly associated with IR (7). NAFLD and NASH also predispose to liver failure and liver cancer, and are leading causes of organ transplantation in North America, with no approved pharmacological therapies (8).

The underlying mechanisms linking fatty liver, inflammation and IR are largely unknown. Human NAFLD has been associated with enhanced pro-inflammatory cytokine markers,

including tumor necrosis factor (TNF) α , interleukin (IL)-1 β and IL-6 (9, 10). Early studies have focused primarily on cells of innate immunity as drivers of the inflammatory and morphological changes that arise in fatty livers. For example, NAFLD is characterized by increased hepatic myeloid cells and aberrant release of T helper 1 (Th1) polarizing inflammatory cytokines (11). Ablation of Kupffer cells improves hepatic steatosis, inflammation and metabolic disease (12, 13). However, few studies have examined the effects of diet-induced obesity (DIO) on adaptive immune cell populations within the liver. In mice, NASH promotes an increase in hepatic CD8⁺/CD4⁺ T cell ratio, dictated by dendritic cell function (14). In NASH, there is an imbalance between excess Th1-derived cytokines such as interferon (IFN) γ and a deficiency in Th2-derived cytokines, including IL-4, IL-5, and IL-13 (15). Consistently, in obese pediatric patients, there is a positive correlation between elevated numbers of circulating IFN γ -expressing CD4⁺ T cells and clinical signs of NAFLD (16). Recently, intrahepatic CD4⁺ and CD8⁺ T cells have been implicated in modulating the transition between NASH and liver cancer (17–19), but whether these cells control hepatic IR, whole body glucose intolerance and overall metabolic syndrome is unknown. Furthermore, the mechanisms and immunological signals that support liver inflammation and maintain pathogenic effector immune cell populations during obesity are poorly understood.

Here, we show that high-fat diet (HFD) feeding in a murine model of obesity-related IR and NAFLD induces the expansion of pathogenic intrahepatic CD8⁺ T cells that promote metabolic disease. Intrahepatic CD8⁺ T cell increase is accompanied by an obesity-induced hepatic type I interferon (IFN-I) response that fuels their accumulation and pathological function. In human patients, the frequency of intrahepatic CD8⁺ T cells positively correlates to glycated hemoglobin (HbA1c) levels. Moreover, intrahepatic CD8⁺ T cells and the presence of intrahepatic IFN-I expression associates with NAFLD disease activity. Thus, DIO promotes an IFN-I response that drives metabolically activated intrahepatic T cell pathogenicity resulting in NAFLD progression and glucose dysregulation.

RESULTS

Obesity Induces a Pro-inflammatory Shift in Intrahepatic T cell Populations

To address the effects of obesity on hepatic immune cell populations, we first investigated whether adaptive immune cells within the liver are altered by HFD (60%kcal fat) feeding in C57BL/6 (WT) mice for 16 weeks. Compared with normal chow diet (NCD)-fed mice, HFD-fed mice showed worsened glucose, insulin and pyruvate tolerance tests (Fig. S1A), increased content of triglycerides in the liver (Fig. S1B), and a substantial increase in the number of total CD3⁺ T cells in the liver (Fig. 1A). Within the CD3⁺ T cell compartment, HFD-fed mice displayed increased frequency of intrahepatic CD8⁺ T cells, a reduction in the frequency of CD4⁺ T cells, and no changes in the frequencies of $\gamma\delta$ TCR⁺ T cell or CD4⁺ Foxp3⁺ T regulatory cells (Fig. 1B, left). However, quantification of cell number per gram of liver tissue revealed that HFD-feeding increased all these intrahepatic T cell subsets, with the greatest increase observed in the CD8⁺ T cell compartment (Fig. 1B, right). HFD-fed mice showed a decrease in hepatic CD1d-restricted invariant NKT cells, as indicated by α -galactosylceramide (α GC)-loaded CD1d tetramer staining (Fig. S1C), while the

frequency and number of NK cells increased (Fig. S1D). No differences in the frequency and number of splenic T cell subsets were found between NCD- and HFD-fed mice (Fig. S1, E and F). Compared with NCD, HFD-feeding markedly increased the frequency and cell number of intrahepatic CD8⁺ CD62L⁻ CD44⁺ T effector memory cells, while no changes in intrahepatic CD4⁺ CD62L⁻ CD44⁺ T effector memory cells were detected (Fig. 1C). In the spleen, we found no differences in the expression of activation markers in CD8⁺ and CD4⁺ T cells between NCD- and HFD-fed mice (Fig. S1G). Additionally, intrahepatic CD8⁺ T cells in HFD-fed mice were mainly CD8 $\alpha\beta$ ⁺ T cells, and no differences in the proportion of CD8 $\alpha\alpha$ ⁺ or CD8 $\alpha\beta$ ⁺ cells were found compared to NCD-fed mice (Fig. S1H).

We next assessed if T cell changes occurred in the liver specific to HFD-induced obesity or if they occur in another model of obesity, the ob/ob mouse, which are genetically obese on NCD. Similar to HFD-fed mice, ob/ob mice showed increased frequency and number of intrahepatic CD8⁺ T cells, and reduced frequency of CD4⁺ T cells, compared with WT controls (Fig. S1, I and J). Differences in T cell subpopulations in the spleen were not observed between ob/ob and WT mice (Fig. S1K).

Given the striking increases in intrahepatic T cells in the HFD model, we investigated mechanisms of increased T cell numbers in the liver. We assessed T cell proliferation by staining for Ki-67, and through use of 5-Ethynyl-2'-deoxyuridine (EdU) uptake. Intrahepatic CD8⁺ and CD4⁺ T cell subsets in HFD-fed mice had increased percentages of Ki-67⁺ cells, and EdU⁺ cells, compared with NCD-fed controls (Fig. 1, D and E), suggesting that HFD-feeding promotes the proliferation of intrahepatic T cells.

To assess the potential of intrahepatic T cell subsets to produce pro-inflammatory cytokines in response to HFD-feeding, we determined their intracellular expression of IFN γ and TNF α . Compared with NCD-fed controls, 16 week HFD-fed mice showed increased frequency and numbers of IFN γ ⁺ CD8⁺, CD4⁺ and $\gamma\delta$ TCR⁺ T cells (Fig. 1F). Similarly, HFD-feeding increased the frequency and number of intrahepatic TNF α ⁺ CD8⁺ and $\gamma\delta$ TCR⁺ cells, although no changes were detected in TNF α ⁺ CD4⁺ T cells (Fig. 1G). Ob/ob mice also showed a higher frequency and number of intrahepatic IFN γ ⁺ CD8⁺ T cells (Fig. S2A), as well as increased frequency of IL-17⁺ $\gamma\delta$ TCR⁺ T cells, compared with WT controls (Fig. S2 B). However, no differences in intrahepatic IL-17⁺ CD4⁺ or $\gamma\delta$ TCR⁺ T cells were found between NCD- and HFD-fed mice (Fig. S2C). In the spleen of HFD-fed mice, CD4⁺, but not CD8⁺, T cells had increased Ki-67 positivity (Fig. S2D) and intracellular expression of IFN γ during HFD-feeding (Fig. S2E), suggesting that there may be some systemic activation of CD4⁺ T cells during HFD feeding, though its changes are relatively small compared with the marked T cell inflammatory changes in the liver. No differences in splenic TNF α ⁺ CD8⁺ T cells were found (Fig. S2F).

To determine the timing of hepatic T cell infiltration over the course of HFD feeding, we analyzed the T cell populations in mice fed a NCD or HFD for shorter (10 weeks) and longer (32 weeks) duration. Although mice fed a HFD for 10 weeks had worsened glucose, insulin and pyruvate tolerance tests (Fig. S3A), as well as increased liver triglycerides (Fig. S3B), these changes were less severe compared to 16 weeks of HFD (Fig. S3C). At 10 weeks of HFD, we detected no significant differences in the frequency and only near

significant trends to increased numbers of intrahepatic T cell subsets (Fig. S3, D and E). By 32 weeks of HFD feeding the increase in the intrahepatic CD8⁺ T cell subsets, including CD8⁺ CD62L⁻ CD44⁺ T effector memory cells, and increased frequency and number of IFN γ ⁺ CD8⁺ and CD4⁺ T cells was exacerbated (Fig. S3, F–I). These results indicate that T cell-derived hepatic inflammation occurs between 10 and 16 weeks of HFD, and worsens thereafter. The findings are consistent with a role for CD8⁺ T cells in exacerbating metabolic disease at these time points.

VAT resident T cells express biased T cell Receptor (TCR) repertoires during DIO, suggesting the potential presence of active antigen-driven immune responses (3, 4). Thus, we next investigated whether similar features are characteristic of intrahepatic T cells during DIO. Analysis of TCRV β expression on total intrahepatic or splenic CD8⁺ and CD4⁺ T cells revealed unremarkable differences between HFD and NCD-fed mice (Fig. S4, A and B). These results suggest that expanded T cells are of unbiased repertoires, and may potentially accumulate through bystander expansion, though a central role for antigen-specific immunity driving T cell accumulation cannot be entirely ruled out. Collectively, our results demonstrate a pro-inflammatory shift in various T cell subsets in the livers of HFD-fed mice, with a notably large increase in the frequency and number of IFN γ - and TNF α -producing CD8⁺ T cells.

To determine if there is an association between intrahepatic T cells and glucose dysregulation in humans, we assessed the frequency of intrahepatic immune cells in a cohort of human liver donor tissues (20). A mixed population of liver donors with varying degrees of body mass index (BMI), fatty liver changes (without NASH), and glucose dysregulation were analyzed for intrahepatic immune cell subsets by flow cytometry, and correlated to BMI and HbA1c. Of all immune cell populations analyzed, only intrahepatic CD8⁺ T cell populations significantly positively correlated with HbA1c levels (Fig. 1H), though there was no significant correlation between CD8⁺ T cells and BMI (Fig. 1I). CD4⁺ T cells (Fig. 1, H and I), and a panel of other immune cell subsets did not positively correlate significantly with BMI or HbA1c levels (Fig. S5, A and B). These findings suggest that intrahepatic CD8⁺ T cells are associated with glucose dysregulation in this cohort of humans, supporting a potential pathogenic role of intrahepatic CD8⁺ T cells in human glucose homeostasis.

Intrahepatic CD8⁺ T cells Drive Hepatic Insulin Resistance and Metabolic Disease

We next investigated if intrahepatic CD8⁺ T cells play a role in the pathogenesis of fatty liver and hepatic IR during DIO, as hepatic insulin signaling is required for normal whole body glucose homeostasis (1). Compared with wild type (WT) controls, CD8-deficient (CD8^{-/-}) mice fed a HFD for 16 weeks displayed only marginal improvements in fatty liver changes, as demonstrated by a trend to decreased liver triglyceride content and overall subtle changes in macrovesicular steatosis observed on H&E sections (Fig. 2A). Despite similar body weight (Fig. 2B), HFD-fed CD8^{-/-} mice had improved systemic insulin sensitivity as shown by a glucose tolerance test (GTT) and insulin tolerance test (ITT), compared with WT controls (Fig. S6A). As increased hepatic IR leads to enhanced hepatic glucose production through activation of gluconeogenic pathways, Pyruvate Tolerance Tests (PTT)

were performed to determine the degree of hepatic IR and gluconeogenesis activity in HFD-fed CD8^{-/-} mice. HFD-fed CD8^{-/-} mice displayed improved overall pyruvate tolerance, compared with WT HFD-fed mice (Fig. 2B). HFD-fed CD8^{-/-} mice also showed reduced mRNA expression of genes that encode the key gluconeogenic enzymes *G6Pc* and *Pepck1* in liver lysates (Fig. 2C), suggesting that CD8⁺ T cells play a role in regulating hepatic glucose production by modulating hepatocyte gluconeogenesis. No differences in gene expression of the lipogenic genes *Srebp1* and *Pparγ* were detected, reflecting the marginal changes observed in histology (Fig. 2A and C). To determine whether intrahepatic CD8⁺ T cells are essential for liver damage in our model of HFD feeding, we measured the serum concentrations of ALT/AST and assessed apoptosis of hepatocytes and liver tissue by TUNEL assay and active caspase-3 in HFD-fed CD8^{-/-} mice. Compared with WT controls, HFD-fed CD8^{-/-} mice showed similar levels of ALT/AST (Fig. S6B) and only non-significant trends to reduced apoptosis (Fig. S6, C–E) suggesting that CD8⁺ T cells are not essential for liver injury in mice fed a HFD at this time point.

Next, to determine the direct effect of intrahepatic CD8⁺ T cells on whole body glucose homeostasis and hepatic glucose production, we adoptively transferred purified liver or splenic CD8⁺ T cells from HFD-fed WT donor mice into HFD-fed CD8^{-/-} recipient mice and performed GTT, ITT, and PTT. Interestingly, transfer of splenic CD8⁺ T cells induced marginal effects on the metabolic parameters measured compared to PBS alone, while transfer of isolated liver CD8⁺ T cells induced a marked worsening of glucose metabolic parameters (Fig. 2D). To further confirm our insulin tolerance studies, we measured the protein levels of total and pAkt in liver tissue of adoptively transferred mice. Compared with PBS treated controls, both liver CD8⁺ and splenic CD8⁺ T cell transfers impaired insulin signaling in liver tissue as determined by lower pAkt/Akt ratios, although liver CD8⁺ T cell transfers had a greater effect (Fig. 2E). A greater percentage of CD8⁺ T cells reconstituted recipient liver tissue, as opposed to VAT or spleen, in liver CD8⁺ T cell transfers (Fig. 2F). Liver CD8⁺ T cell transfers displayed a greater proportion of activated CD62L⁺ CD44⁺ T effector memory subsets, which may be one reason for their enhanced pathogenicity compared with splenic CD8⁺ T cell transfers (Fig. 2F).

Collectively, these data suggest that hepatic CD8⁺ T cells are a unique, highly pathogenic tissue-specific immune mediator of obesity-related glucose dysregulation. Moreover, the pathogenicity of hepatic CD8⁺ T cells is in part linked to modulation of hepatocyte gluconeogenesis, which is a process augmented by hepatic IR. Given the large increases in pro-inflammatory cytokine production observed in these cells, such processes may potentially occur through the release of IFN γ and TNF α , which impair insulin receptor signaling in several tissues (1, 21). Thus, we treated primary hepatocytes with IFN γ , TNF α , or both, to investigate their effects on insulin signaling. Treatment of hepatocytes with IFN γ , TNF α , or both reduced pAkt/Akt protein ratios compared to untreated cells (Fig. 2G). The results support the notion that typical inflammatory cytokines produced by CD8⁺ T cells impair downstream insulin signaling in the liver.

HFD-feeding Induces a Type I Interferon Response in the Liver that Promotes Insulin Resistance

Given that intrahepatic CD8⁺ T cells show important pathological functions on glucose homeostasis, we next investigated potential immunological mechanisms governing the activation and persistence of pro-inflammatory intrahepatic T cells observed in HFD-fed mice. IFN-I are critical for the survival, memory, effector differentiation, proliferation and cytolytic activity of T cells during various settings, including infection (22). IFN-I responses, driven by IFN α and IFN β , are transcriptionally regulated by interferon regulatory factors (IRFs) and are induced following pathogen recognition by pattern-recognition receptors (23). Secreted IFN-I signal through the interferon α receptor (IFN α R) to induce the expression of interferon stimulatory genes (ISGs). We examined whether HFD-feeding results in an IFN-I response that fuels the activation of intrahepatic T cells during DIO. Compared with NCD controls, HFD-fed mice showed enhanced hepatic expression of *IRF3* and *IRF7*, key transcription factors involved in the regulation of IFN-I responses, as well as several ISGs, including *ISG15*, *IFIT1*, and *IFI44* (Fig. 3A, left). Livers from HFD-fed mice also had increased expression of IFN α R in a number of immune cells, including CD8 T cells (Fig. S6F), as well as higher contents of IFN α protein (Fig. 3A, right). To examine the relative contribution of several intrahepatic immune cells to the increased response to IFN-I, we determined the expression of ISGs in CD8⁺, CD4⁺, and CD11b⁺ cells purified from the liver of NCD- and HFD-fed mice. Compared with NCD, livers from HFD-fed mice had increased expression of *ISG15*, *IFIT1*, *IFI44*, and *USP18* in purified CD8⁺ T cells (Fig. 3B), and *USP18* in CD11b⁺ cells (Fig. S6G, **top**). No differences were detected in the expression of ISGs between NCD- and HFD-fed mice in purified CD4 T⁺ cells (Fig. S6G, **bottom**). We further confirmed increased expression of one ISG, *ISG15*, in CD8⁺ T cells using RNA fluorescent in situ hybridization (FISH) followed by branched amplification and flow cytometry analysis (PrimeFlow®) (Fig. S6H). Together, these results demonstrate that HFD-feeding promotes an active IFN-I response in the liver that is strongly localized to CD8⁺ T cells.

We next investigated whether IFN-I responses have a major role in obesity-related IR by assessing metabolic parameters of IFN α R1-deficient (IFN α R1^{-/-}) mice fed a HFD. Histological analysis of H&E liver stains from 16 week HFD-fed IFN α R1^{-/-} mice revealed these mice were protected from fatty liver, with reductions in microvesicular and macrovesicular steatosis compared to WT HFD-fed controls (Fig. 3C, left). This finding was consistent with reduced liver weight (Fig. 3C, middle), triglyceride content (Fig. 3C, right), and lipid content observed by oil red O staining (Fig. S7A) in IFN α R1^{-/-}-HFD-fed mice, while no differences in adipose tissue weight (Fig. 3D, left) or total body weight (Fig. 3D, right) were found. Compared to WT HFD-fed control mice, HFD-fed IFN α R1^{-/-} mice were protected from DIO-related IR, as determined by improved GTTs, ITTs, and PTTs (Fig. 3E), and reduced plasma fasting glucose and insulin levels (Fig. 3F). This protection was dependent on HFD-feeding, as NCD-fed IFN α R1^{-/-} mice displayed no differences in the metabolic tests performed, compared with WT controls (Fig. S7, B–D). These data suggest that factors present in a HFD or obese settings promote pathogenic IFN-I responses. To further confirm IR in the liver, we measured protein levels of total and pAkt after insulin

challenge, and consistent with our findings, IFN α R1^{-/-} HFD-fed mice displayed higher levels of pAkt/Akt ratios compared with WT HFD-fed controls (Fig. 3G).

We then investigated if intrahepatic T cells relied on IFN-I cytokines for their activation and accumulation. IFN α R1^{-/-} HFD-fed mice exhibited lower total intrahepatic CD8⁺ and CD4⁺ T cells (Fig. 3H), with no significant differences observed in the spleen (Fig. S7E). Remarkably, the frequency and total number of CD62L⁻ CD44⁺ T effector memory CD8⁺ and CD4⁺ T cell subsets were strikingly decreased in IFN α R1^{-/-} HFD-fed mice, similar to levels observed in NCD-fed mice (Fig. 3H and 1C). Ki-67⁺ CD8⁺ and CD4⁺ intrahepatic T cells were also reduced in IFN α R1^{-/-} HFD-fed mice (Fig. 3I), suggesting that IFN-I promotes the proliferation of intrahepatic T cells. Upon stimulation, intrahepatic T cells from IFN α R1^{-/-} HFD-fed mice displayed marked decreased frequencies and cell numbers of IFN γ ⁺ CD8⁺ and CD4⁺ cells (Fig. 3J). Although no differences were detected in the percentages of TNF α ⁺ CD8⁺ and CD4⁺ T cells, IFN α R1^{-/-} HFD-fed mice showed a decrease in the number of TNF α ⁺ CD8⁺ intrahepatic T cells (Fig. 3K). While no changes in splenic IFN γ ⁺ CD8⁺ T cells were observed (Fig. S7F), splenic CD8⁺ TNF α ⁺ (Fig. S7G) and CD8⁺ T effector memory cells (Fig. S7H) were also found to be marginally reduced in IFN α R1^{-/-} HFD-fed mice. Overall, these findings suggest that IFN-I responses fuel the proliferation and activation of intrahepatic T cells, leading to an increased release of pathogenic inflammatory cytokines during DIO.

Since we identified IFN-I as a dominant central process governing glucose homeostasis in knockout mice, we next assessed whether reducing IFN-I through an IFN α R1 blocking antibody after established metabolic disease could have therapeutic potential. We treated 10 week HFD-fed mice with either 400 μ g/week of anti-IFN α R1 antibody, or IgG control for 5 weeks and metabolic testing was performed. Despite no changes in body weight, mice receiving anti-IFN α R1 blocking antibody showed improved glucose tolerance, insulin sensitivity, and pyruvate tolerance at the end of the treatment course (Fig. 4A). IFN α R1 blocking was confirmed by flow cytometry and improved disease correlated with reduced total intrahepatic CD8⁺ and CD4⁺ T cells, and decreases in T effector memory populations (Fig. 4B). Together, these data suggest that IFN-I responses represent a critical immunological mechanism for the expansion and proliferation of activated pro-inflammatory intrahepatic T cells observed during HFD-feeding.

Given that IFN-I responses can control intrahepatic immune populations and glucose metabolism, we next sought out possible sources of IFN-I production in DIO. Obesity-associated changes in the gut microbiota control inflammation and IR partly through increased gut-derived bacterial products, such as lipopolysaccharide (LPS) and unmethylated CpG DNA (24, 25), which have been also shown to regulate the progression of NAFLD (26). Because the liver receives direct drainage of blood containing food and bacterial antigens from the gut, we questioned if such products could induce hepatic IFN-I production. We treated primary hepatocytes isolated from WT mice with LPS (TLR4 agonist) or unmethylated CpG/ODN2395 (TLR9 agonist). Compared with untreated controls, both LPS and CpG ODN increased the expression of *IRF3*, while CpG ODN treatment resulted in higher expression of *IRF7* (Fig. S8A). These results suggest that such bacterial products within liver tissue may be one potential inducer of the IFN-I responses.

Saturated free fatty acids have also been identified to contribute to the development of fatty liver disease in TLR2 and TLR4 dependent manners (27). While IRF7 showed a trend to increased expression with high dose palmitate, overall we found no significant differences in *IRF3* and *IRF7* gene expression in hepatocytes stimulated with palmitate (Fig. S8B).

To identify whether increased liver IFN-I responses and intrahepatic T cell inflammation during DIO is driven by intestinal bacterial components, we depleted WT HFD-fed mice of commensal bacteria by oral administration of broad spectrum antibiotics (28). Compared with controls, WT antibiotic-treated mice showed a dramatic improvement in a GTT, ITT, and PTT (Fig. S8 C–E), reduced IFN α in the liver (Fig. S8F), and reduced numbers of intrahepatic CD8⁺ T cells (Fig. S8G) and CD8⁺ T effector memory cells (Fig. S8H). To determine if the improvement in metabolic parameters observed in antibiotic-treated mice is IFN-I dependent, we treated HFD-fed IFN α R1^{-/-} mice with antibiotics and performed metabolic testing. In contrast to WT mice, IFN α R1^{-/-} antibiotic-treated mice only showed marginal improvements in glucose testing (Fig. S8, C–E) and no changes in the number of intrahepatic CD8⁺ T cells (Fig. S8I), compared with IFN α R1^{-/-} controls. This finding is consistent with the notion that IFN-I responses mechanistically promote some of the detrimental effects of bacteria on glucose metabolism during HFD-feeding. Together, these data suggest that bacterial products can up-regulate IFN-I responses in the liver, and that these changes are associated with intrahepatic T cell inflammation during obesity.

Loss of Type I Interferon Signaling on Intrahepatic T cells Protects from Metabolic Disease

Since we have shown that intrahepatic CD8⁺ T cells possess pathogenic properties in modulating glucose metabolism, and that these cells are maintained by a IFN-I response, we next assessed the metabolic effects of disrupted IFN-I signaling in CD8⁺ T cells alone during DIO through use of mixed bone marrow chimeric mice (29). Irradiated recipient mice were reconstituted with bone marrow mixtures containing 85%:15% ratios of either CD8^{-/-} bone marrow + IFN α R1^{-/-} bone marrow (IFN α R1^{-/-} CD8), or CD8^{-/-} bone marrow + WT bone marrow (WT CD8) and then were placed on a HFD for 16 weeks. Despite no changes in body weight, chimeric mice lacking IFN α R1 on CD8⁺ T cells (IFN α R1^{-/-} CD8) displayed better overall glucose tolerance, insulin sensitivity and pyruvate tolerance compared to control counterparts (WT CD8) (Fig. 4C). The absence of IFN α R1 expression on CD8⁺ T cells in IFN α R1^{-/-} CD8 mice was confirmed by flow cytometry (Fig. 4D). Interestingly, IFN α R1^{-/-} CD8 HFD-fed chimeric mice displayed reduced total intrahepatic CD8⁺ T cells, and decreased CD8⁺ CD62L⁻ CD44⁺ and CD4⁺ CD62L⁻ CD44⁺ T effector memory cells (Fig. 4E). These findings pinpoint IFN-I-IFN α R1 signaling in intrahepatic CD8⁺ T cells as an important mechanism promoting their accumulation and pathologic function in DIO.

Human Fatty Liver Disease Activity Correlates with Increased CD8⁺ T cell Infiltration and Type I Interferon Responses

To assess clinical relevance of CD8⁺ T cell and IFN-I responses in human livers, we measured CD8⁺ T cell infiltration and IFN-I responsive proteins in human liver biopsies from patients with varying degrees of NAFLD. Histological sections were given a NAFLD Activity Score (NAS) ranging from low disease (NAS 0) to advanced steatohepatitis (NAS

8) (30) and immunohistochemical stains were evaluated by the staining intensity and tissue percentage stained. Consistent with our mouse data, we found a significant positive correlation between NAS score and IRF3 or ISG15 protein expression throughout human liver sections (Fig. 4, F and G). In addition to IRF3 and ISG15 expression, NAS score correlated with increased CD8⁺ infiltration in lobules and portal tracts of liver tissue (Fig. 4H). These data suggest that human fatty livers display elevated IFN-I responses and CD8⁺ T cell infiltration, and may serve as potential biomarkers, or targets in the treatment of disease.

DISCUSSION

NAFLD and associated IR mainly have been linked to innate immunity whereby activation of TLRs, NF κ B and the inflammasome in the liver promote disease. Our results highlight mechanisms by which DIO fuels hepatic inflammation through initiation of an IFN-I response that supports accumulation of CD8⁺ T cells that result in worsened overall glucose homeostasis. Hepatic CD8⁺ T cells likely represent a unique, highly pathogenic tissue-specific mediator of obesity-related glucose dysregulation. Using several methods, we identified that CD8⁺ T cells promote glucose dysregulation by augmenting hepatic IR and gluconeogenesis. It is likely that hepatic CD8⁺ T cells induce their insulin desensitizing effects through release of IFN γ and TNF α which impair insulin signaling in hepatocytes. In addition, TNF α has also been associated with fibrosis in NASH (9). While our data points to T cell derived IFN γ and TNF α mediated pathology, several studies have found that IL-17 also may be important in the pathogenesis of NAFLD (31–33). Discrepancies surrounding the roles of IL-17 may be due to differences in the inciting model of NAFLD, lineage plasticity within Th17 populations, or microbial variability between facilities, which dictate Th17 responses (34).

Although TCRV β analysis of liver T cells during HFD-feeding did not reveal remarkable differences, the nature of T cell responses in the liver as a result of antigen-directed or bystander responses requires further investigation. In fact, an expanding list of antigen targets are being reported for obese, IR individuals, and an autoimmune, or antigen-driven component to obesity-related IR has been debated (35).

We next identified a fundamental role for IFN-I responses in driving hepatic T cell inflammation and metabolic disease. Consistent with other recent reports, we identified enhanced hepatic gene expression of key IFN-I regulatory factors, *IRF3* and *IRF7*, during DIO and/or NAFLD, (36, 37). While previous studies used knock-out mice to examine the role of individual IRFs associated with IFN-I pathways and their effects on glucose metabolism (36, 38, 39), we utilized HFD-fed IFN α R1 knock-out mice to broadly eliminate IFN-I and showed that IFN-I responses, as a whole, promote obesity-related IR. A recent study reported that deletion of IFN α R1 in adipocytes of HFD-fed mice resulted in worsened steatosis and metabolic parameters, whereas no differences were detected when IFN α R1 was deleted in hepatocytes, intestinal epithelial cells, and myelocytes, compared with WT controls (40). Combined with our data, these findings would still support a dominant pathogenic role for IFN α R1 in lymphocytes, such as CD8⁺ T cells, that result in systemic IR. Interestingly, IFN-I responsive CD8⁺ T cells appear to effect the activation status of

CD4⁺ T cells, as CD8⁺ IFN α R1^{-/-} chimeric mice were found to have reduced CD4⁺ T cell subsets. This finding suggests that CD8⁺ T cells may play a fundamental role in orchestrating inflammation in fatty livers, similar to their role in VAT inflammation. Alternatively, IFN-I may impair hepatocyte insulin signaling directly (41). Recent studies show that IFN-I can cause direct oxidative damage to hepatocytes, and induces fatty acid uptake in cells, including macrophages (42, 43).

IFN-I responses are typically induced by RNA or DNA viruses through the endosomal TLR7/8/9, but can also be stimulated through other TLRs, including TLR4 (23, 44). Multiple mechanisms may contribute to the increased IFN-I response in the livers of HFD-fed mice. It is possible that hepatic IFN-I responses are induced by increased bacterial products entering liver tissue due to increased intestinal permeability (45). Here, we show that livers of HFD-fed microbiota-depleted mice have reduced IFN α and CD8⁺ T cells, suggesting that commensal-derived ligands may be a source of antigens driving hepatic IFN-I and T cell responses. Similarly, mice treated with broad-spectrum antibiotics display decreased infiltration of intrahepatic macrophages during HFD feeding (46). In addition to bacterial sources of antigenic stimulants, mitochondrial DNA from hepatic origin is increased in mice and patients with NASH (47), which could act as TLR9 ligands to promote IFN-I production. Other factors that might induce IFN-I responses in the liver include dietary fats, though our *in vitro* data for two dominant IRFs did not reach significance after addition of palmitate. Hepatocytes or IFN-I-producing intrahepatic immune cells, including plasmacytoid dendritic cells (pDCs), may be sources of IFN-I production which contribute to hepatic inflammation in obesity (48).

Although we propose CD8⁺ T cells to be a dominant IFN-I responsive cell driving our observed results, several other IFN-I responsive immune cells may play a role. HFD-fed whole-body IFN α R1^{-/-} mice were more protected against HFD-induced glucose dysregulation than CD8-specific IFN α R1^{-/-} mice, suggesting that there may be other cellular subsets that require IFN-I signalling to promote disease progression. Nonetheless, we identified strong IFN-I signaling patterns within purified intrahepatic CD8⁺ T cells. As well, while we identified increases in protein levels of IFN α in the liver, the relative contributions of the major IFN-I effector cytokines, IFN α and IFN β , remain to be determined, especially since IFN β can exert anti-inflammatory effects in some models of disease (49). Moreover, long standing IFN-I signaling is associated with immune exhaustion in models of persistent viral infection (50). It will be interesting to assess the role of this cytokine axis in long standing persistent metabolic disease as a mechanism of immunosuppression. Furthermore, we cannot entirely rule out a contributory role for IFN-I in modulating VAT inflammation in addition to the liver, as the etiology of NAFLD involves adipose-derived inflammatory mediators, including FFAs and cytokines (5). A recent study reported that IRF3 expression in adipose tissue supports IR by promoting macrophage-mediated VAT inflammation and repressing browning of fat, while another study linked IFN-I responses in VAT to IR in a human cohort (51, 52). However, the changes we identified during PTTs, and pAkt/Akt expression in the liver do lend support to a mechanism which may impact local hepatic insulin signalling.

The potential clinical relevance of our findings was illustrated using two different human liver cohorts. While both hepatocytes and immune cells displayed positive staining for IRF3 and ISG15 protein in human liver sections, further investigation is warranted to delineate the relative contribution of each cell type. Furthermore, the use of IFN-I-related proteins, or CD8⁺ T cell infiltration as possible future diagnostic markers of NAFLD or NASH disease is also an avenue of future investigation. Lastly, given the central role IFN-I has in mediating anti-viral responses (53, 54), additional clinical studies on the safety and efficacy of manipulating IFN-I responses for the treatment of obesity-related metabolic abnormalities is required.

Overall, our work identifies an IFN-I signaling axis as a central immunological pathway driving T cell mediated liver inflammation during DIO. This notion identifies IFN-I as a common immunological hub shared with other liver diseases in which IFN-I signaling plays an important role, including infectious hepatitis (55, 56). Collectively, our findings identify IFN-I and its responsive intrahepatic T cell subsets are important elements of metabolic syndrome pathobiology, including NAFLD and IR. Our observations give insight into metabolic disease, and propose new avenues for therapeutic strategies to combat the growing obesity epidemic and its associated metabolic abnormalities.

MATERIALS AND METHODS

Study design

The aim of this study was to investigate whether intrahepatic T cell populations promote IR and glucose intolerance during obesity, and to determine factors, including IFN-I, that maintain these cells within metabolic tissues. All animal studies were performed under the approval of Animal User Protocols by the Animal Care Committee at the University Health Network. For approval of human studies, please see specific section in the Methods. See Supplemental Experimental Procedures (SEP) for full details on study design.

Mice

C57BL/6J (WT), C57BL/6J leptin deficient ob/ob (ob/ob), CD45.1 (B6.SJL-*Ptprc^a Pepc^{bj}*/BoyJ), CD8^{-/-} (B6.129S2-*Cd8a^{tm1Mak}*/J), and IFN α R1^{-/-} (B6.129S2-*Ifnar1^{tm1Ag1}*/Mmjax) mice were purchased from Jackson Laboratory. Heterozygous mice were crossed to generate C57BL/6J wild type (WT) and IFN α R1^{-/-} littermates. Mice were fed either NCD (15 kcal % fat), or HFD (Research Diets, 60 kcal % fat, irradiated) starting at 6 weeks of age for 16–32 weeks. See SEP.

Metabolic Studies

Glucose and insulin testing were performed as previously described (57). For PTTs, mice were fasted for 16 hours and then injected intraperitoneally (i.p.) with 1.5 g/kg (of body weight) of sodium pyruvate (Sigma) in PBS. Liver triglyceride contents were determined using a colorimetric assay (Cayman Chemical). See SEP.

Processing of immune cells from tissues

All tissue was weighed before processing. Immune cells were isolated from liver, VAT and spleen as previous described (48). See SEP.

Flow Cytometry

Cells were stained with commercial fluorophore-conjugated primary antibodies listed in Supplemental Table 1 using recommended dilutions from the supplier (Biolegend). See SEP.

Mixed Bone Marrow Chimeras

Mixed bone marrow (BM) chimeric mice were generated using a modified protocol as described (29). See SEP.

Anti-IFN α R1 Treatment

Ten week HFD-fed WT mice were injected i.p. with 400 μ g of either anti-IFN α R1 blocking antibody (InVivoMAb, clone MAR1-5A3) or mouse IgG1 isotype control (InVivoMAb, clone MOPC-21) in 100 μ l PBS once per week for 5 weeks. Metabolic tests were performed after the end of treatment course and IFN α R1 blocking was evaluated by flow cytometry.

In vivo incorporation of EdU

Mice were injected i.p. with 4 μ g/g body weight of 5-Ethynyl-2'-deoxyuridine (EdU, Invitrogen) and their liver and spleens were collected 48 hours later. Intracellular EdU was labeled with Alexa Fluor 488 in a Click-iT reaction (Invitrogen) according to the manufacturer's protocol and measured by flow cytometry.

Cell Transfer Experiments

Hepatic immune cells or splenocytes from 16–20 week HFD-fed mice were isolated and CD8⁺ T cells were purified (>95%) using an Easy Sep Negative Selection Kit (StemCell Technologies Inc.). Sixteen week HFD-fed CD8^{-/-} mice received 5 \times 10⁶ hepatic or splenic CD8⁺ T cells intravenously in 100 μ l PBS and metabolic studies were performed 1 week after transfer.

Depletion of Intestinal Commensal Bacteria

Mice fed a HFD for 12 weeks were received a combination of ampicillin (1 g/L, Sigma), vancomycin (0.5 g/L, Sigma), neomycin (1 g/L, Sigma), and metronidazole (1 g/L, Sigma) in the drinking water for 4 weeks, as previously described (28).

Treatment of Primary Hepatocytes

Primary hepatocytes were isolated from 6–8 week old NCD-fed WT mice as described (58). Cells were then treated with 20 ng/ml recombinant IFN- γ or TNF- α (BioLegend), 0.1 and 1 μ g/ml LPS-EK (InvivoGen), 1 and 10 μ g/ml ODN2395 (InvivoGen), or 0.5 and 1.0 mM sodium palmitate (Sigma) for 12 or 24 hours. For pAkt/Akt western blotting studies, cells were treated with 100 nM of insulin (Eli Lilly) for 15 minutes. See SEP.

Western Blotting

Western blotting was performed as previously described (57). See SEP.

RNA isolation and Quantitative Real Time-PCR

Primer sets are listed in Supplemental Table 2. Changes in gene expression were calculated by the $2^{-C(T)}$ method using mean cycle threshold (CT) values as described (57). Expression of GAPDH did not change between groups and results are shown as fold changes relative to the control group. See SEP.

Histology and Human Liver Biopsies

For human studies, a cohort of 19 human liver biopsies taken from patients with varying degrees of NAFLD and NASH were sectioned and 18 were stained for hematoxylin, anti-human CD8 (Abcam, clone 144B), and anti-human ISG15 (Abcam, clone EPR3445), and 19 for anti-human IRF3 (Abcam, clone EPR2418Y) that were detected using an ImmPRESS kit (Vector labs) followed by chromogen exposure as described (25). All histochemical and immunohistochemical stains were performed by the UHN Pathology Research Program (PRP) labs at UHN. All human specimens were obtained with study approval by the Research Ethics Board for Human Subjects at the University Health Network. See SEP.

Isolation of Human Intrahepatic Mononuclear Cells

Liver-associated mononuclear cells were isolated from the liver of cadaveric donors (n=30) at Mid-American Transplant Services for organs assigned for transplant at Saint Louis University Hospital or Barnes Jewish Hospital Abdominal Transplant Programs. The patient cohort consisted of 18 males and 12 females with an average age of 43.57. HbA1c was measured and available for 21 patients and analysis of intrahepatic immune cell subsets was performed by flow cytometry as described (20, 59). The study was approved by Saint Louis University and informed consent was provided by next-of-kin. See SEP.

Statistical Analysis

Statistical significance between two means was assessed with an unpaired, two-sided Student's t test using GraphPad Prism5 (GraphPad Software, Inc.). In figure legends, where specified, the number of biological experiments is listed as the n value. All data represent mean \pm standard error of the mean (SEM). Spearman rank correlation coefficient tests were performed to analyze correlative studies. Statistical significance is denoted by * = p<0.05, ** = p<0.01, *** = p<0.001. Statistical significance was set at p < 0.05.

Supplementary Material

Refer to Web version on PubMed Central for supplementary material.

Acknowledgments

We thank Dr. Pamela Ohashi for discussing results. All other authors discussed results and/or reviewed the manuscript.

FUNDING

This work was supported in part by Canadian Institutes of Health Research (CIHR) grants 119414, 132562, 142708, and 148385 (D.A.W.); Canadian Diabetes Association (CDA) grants OG-3-15-5014 and CS-5-12-3886 (D.A.W.); J.P. Bickell Foundation Grant (D.A.W.). D.A.W. received a Canada Research Chair and the Ontario Ministry of Innovation Early Researcher Award. M.G. received a CIHR Canada Graduate Scholarship-Master's. M.K.N. is the recipient of an Alfred Benzon Foundation Postdoctoral Fellowship and X.R. is the recipient of a CDA Postdoctoral Fellowship Award.

References

1. Osborn O, Olefsky JM. The cellular and signaling networks linking the immune system and metabolism in disease. *Nature medicine*. 2012; 18:363–374.
2. Hotamisligil GS, Shargill NS, Spiegelman BM. Adipose expression of tumor necrosis factor- α : direct role in obesity-linked insulin resistance. *Science (New York, NY)*. 1993; 259:87–91.
3. Winer S, Chan Y, Paltser G, Truong D, Tsui H, Bahrami J, Dorfman R, Wang Y, Zielinski J, Mastronardi F, Maezawa Y, Drucker DJ, Engleman E, Winer D, Dosch HM. Normalization of obesity-associated insulin resistance through immunotherapy. *Nature medicine*. 2009; 15:921–929.
4. Nishimura S, Manabe I, Nagasaki M, Eto K, Yamashita H, Ohsugi M, Otsu M, Hara K, Ueki K, Sugiura S, Yoshimura K, Kadowaki T, Nagai R. CD8⁺ effector T cells contribute to macrophage recruitment and adipose tissue inflammation in obesity. *Nature medicine*. 2009; 15:914–920.
5. Haas JT, Francque S, Staels B. Pathophysiology and Mechanisms of Nonalcoholic Fatty Liver Disease. *Annu Rev Physiol*. 2016; 78:181–205. [PubMed: 26667070]
6. Bellentani S, Scaglioni F, Marino M, Bedogni G. Epidemiology of non-alcoholic fatty liver disease. *Dig Dis*. 2010; 28:155–161. [PubMed: 20460905]
7. Fabbrini E, Magkos F, Mohammed BS, Pietka T, Abumrad NA, Patterson BW, Okunade A, Klein S. Intrahepatic fat, not visceral fat, is linked with metabolic complications of obesity. *Proceedings of the National Academy of Sciences of the United States of America*. 2009; 106:15430–15435. [PubMed: 19706383]
8. Wong RJ, Aguilar M, Cheung R, Perumpail RB, Harrison SA, Younossi ZM, Ahmed A. Nonalcoholic steatohepatitis is the second leading etiology of liver disease among adults awaiting liver transplantation in the United States. *Gastroenterology*. 2015; 148:547–555. [PubMed: 25461851]
9. Crespo J, Cayon A, Fernandez-Gil P, Hernandez-Guerra M, Mayorga M, Dominguez-Diez A, Fernandez-Escalante JC, Pons-Romero F. Gene expression of tumor necrosis factor α and TNF-receptors, p55 and p75, in nonalcoholic steatohepatitis patients. *Hepatology*. 2001; 34:1158–1163. [PubMed: 11732005]
10. Wieckowska A, Papouchado BG, Li Z, Lopez R, Zein NN, Feldstein AE. Increased hepatic and circulating interleukin-6 levels in human nonalcoholic steatohepatitis. *Am J Gastroenterol*. 2008; 103:1372–1379. [PubMed: 18510618]
11. Obstfeld AE, Sugar E, Thearle M, Francisco AM, Gayet C, Ginsberg HN, Ables EV, Ferrante AW Jr. C-C chemokine receptor 2 (CCR2) regulates the hepatic recruitment of myeloid cells that promote obesity-induced hepatic steatosis. *Diabetes*. 2010; 59:916–925. [PubMed: 20103702]
12. Huang W, Metlakunta A, Dedousis N, Zhang P, Sipula I, Dube JJ, Scott DK, O'Doherty RM. Depletion of liver Kupffer cells prevents the development of diet-induced hepatic steatosis and insulin resistance. *Diabetes*. 2010; 59:347–357. [PubMed: 19934001]
13. Stienstra R, Saudale F, Duval C, Keshtkar S, Groener JE, van Rooijen N, Staels B, Kersten S, Muller M. Kupffer cells promote hepatic steatosis via interleukin-1 β -dependent suppression of peroxisome proliferator-activated receptor α activity. *Hepatology*. 2010; 51:511–522. [PubMed: 20054868]
14. Henning JR, Graffeo CS, Rehman A, Fallon NC, Zambirinis CP, Ochi A, Barilla R, Jamal M, Deutsch M, Greco S, Ego-Osuala M, Bin-Saeed U, Rao RS, Badar S, Quesada JP, Acehan D, Miller G. Dendritic cells limit fibroinflammatory injury in nonalcoholic steatohepatitis in mice. *Hepatology*. 2013; 58:589–602. [PubMed: 23322710]
15. Maher JJ, Leon P, Ryan JC. Beyond insulin resistance: Innate immunity in nonalcoholic steatohepatitis. *Hepatology*. 2008; 48:670–678. [PubMed: 18666225]

16. Pacifico L, Di Renzo L, Anania C, Osborn JF, Ippoliti F, Schiavo E, Chiesa C. Increased T-helper interferon-gamma-secreting cells in obese children. *Eur J Endocrinol.* 2006; 154:691–697. [PubMed: 16645016]
17. Wolf MJ, Adili A, Piotrowitz K, Abdullah Z, Boege Y, Stemmer K, Ringelhan M, Simonavicius N, Egger M, Wohlleber D, Lorentzen A, Einer C, Schulz S, Clavel T, Protzer U, Thiele C, Zischka H, Moch H, Tschop M, Tumanov AV, Haller D, Unger K, Karin M, Kopf M, Knolle P, Weber A, Heikenwalder M. Metabolic activation of intrahepatic CD8+ T cells and NKT cells causes nonalcoholic steatohepatitis and liver cancer via cross-talk with hepatocytes. *Cancer Cell.* 2014; 26:549–564. [PubMed: 25314080]
18. Ma C, Kesarwala AH, Eggert T, Medina-Echeverez J, Kleiner DE, Jin P, Stroncek DF, Terabe M, Kapoor V, ElGindi M, Han M, Thornton AM, Zhang H, Egger M, Luo J, Felsher DW, McVicar DW, Weber A, Heikenwalder M, Greten TF. NAFLD causes selective CD4(+) T lymphocyte loss and promotes hepatocarcinogenesis. *Nature.* 2016; 531:253–257. [PubMed: 26934227]
19. Gomes AL, Teijeiro A, Buren S, Tummala KS, Yilmaz M, Waisman A, Theurillat JP, Perna C, Djouder N. Metabolic Inflammation-Associated IL-17A Causes Non-alcoholic Steatohepatitis and Hepatocellular Carcinoma. *Cancer Cell.* 2016; 30:161–175. [PubMed: 27411590]
20. Tang XZ, Jo J, Tan AT, Sandalova E, Chia A, Tan KC, Lee KH, Gehring AJ, De Libero G, Bertoletti A. IL-7 licenses activation of human liver intrasinusoidal mucosal-associated invariant T cells. *J Immunol.* 2013; 190:3142–3152. [PubMed: 23447689]
21. Michael MD, Kulkarni RN, Postic C, Previs SF, Shulman GI, Magnuson MA, Kahn CR. Loss of insulin signaling in hepatocytes leads to severe insulin resistance and progressive hepatic dysfunction. *Mol Cell.* 2000; 6:87–97. [PubMed: 10949030]
22. Kolumam GA, Thomas S, Thompson LJ, Sprent J, Murali-Krishna K. Type I interferons act directly on CD8 T cells to allow clonal expansion and memory formation in response to viral infection. *The Journal of experimental medicine.* 2005; 202:637–650. [PubMed: 16129706]
23. Decker T, Muller M, Stockinger S. The yin and yang of type I interferon activity in bacterial infection. *Nat Rev Immunol.* 2005; 5:675–687. [PubMed: 16110316]
24. Cani PD, Bibiloni R, Knauf C, Waget A, Neyrinck AM, Delzenne NM, Burcelin R. Changes in gut microbiota control metabolic endotoxemia-induced inflammation in high-fat diet-induced obesity and diabetes in mice. *Diabetes.* 2008; 57:1470–1481. [PubMed: 18305141]
25. Luck H, Tsai S, Chung J, Clemente-Casares X, Ghazarian M, Revelo XS, Lei H, Luk CT, Shi SY, Surendra A, Copeland JK, Ahn J, Prescott D, Rasmussen BA, Chng MH, Engleman EG, Girardin SE, Lam TK, Croitoru K, Dunn S, Philpott DJ, Guttman DS, Woo M, Winer S, Winer DA. Regulation of Obesity-Related Insulin Resistance with Gut Anti-inflammatory Agents. *Cell metabolism.* 2015; 21:527–542. [PubMed: 25863246]
26. Hena-Mejia J, Elinav E, Jin C, Hao L, Mehal WZ, Strowig T, Thaïss CA, Kau AL, Eisenbarth SC, Jurczak MJ, Camporez JP, Shulman GI, Gordon JI, Hoffman HM, Flavell RA. Inflammation-mediated dysbiosis regulates progression of NAFLD and obesity. *Nature.* 2012; 482:179–185. [PubMed: 22297845]
27. Miura K, Yang L, van Rooijen N, Brenner DA, Ohnishi H, Seki E. Toll-like receptor 2 and palmitic acid cooperatively contribute to the development of nonalcoholic steatohepatitis through inflammasome activation in mice. *Hepatology.* 2013; 57:577–589. [PubMed: 22987396]
28. Rakoff-Nahoum S, Paglino J, Eslami-Varzaneh F, Edberg S, Medzhitov R. Recognition of commensal microflora by toll-like receptors is required for intestinal homeostasis. *Cell.* 2004; 118:229–241. [PubMed: 15260992]
29. Nishimura S, Manabe I, Takaki S, Nagasaki M, Otsu M, Yamashita H, Sugita J, Yoshimura K, Eto K, Komuro I, Kadowaki T, Nagai R. Adipose Natural Regulatory B Cells Negatively Control Adipose Tissue Inflammation. *Cell metabolism.* 2013
30. Kleiner DE, Brunt EM, Van Natta M, Behling C, Contos MJ, Cummings OW, Ferrell LD, Liu YC, Torbenson MS, Unalp-Arida A, Yeh M, McCullough AJ, Sanyal AJ. N. Nonalcoholic Steatohepatitis Clinical Research. Design and validation of a histological scoring system for nonalcoholic fatty liver disease. *Hepatology.* 2005; 41:1313–1321. [PubMed: 15915461]
31. Rau M, Schilling AK, Meertens J, Hering I, Weiss J, Jurowich C, Kudlich T, Hermanns HM, Bantel H, Beyersdorf N, Geier A. Progression from Nonalcoholic Fatty Liver to Nonalcoholic Steatohepatitis Is Marked by a Higher Frequency of Th17 Cells in the Liver and an Increased

- Th17/Resting Regulatory T Cell Ratio in Peripheral Blood and in the Liver. *J Immunol.* 2016; 196:97–105. [PubMed: 26621860]
32. Giles DA, Moreno-Fernandez ME, Stankiewicz TE, Cappelletti M, Huppert SS, Iwakura Y, Dong C, Shanmukhappa SK, Divanovic S. Regulation of Inflammation by IL-17A and IL-17F Modulates Non-Alcoholic Fatty Liver Disease Pathogenesis. *PLoS One.* 2016; 11:e0149783. [PubMed: 26895034]
 33. Harley IT, Stankiewicz TE, Giles DA, Softic S, Flick LM, Cappelletti M, Sheridan R, Xanthakos SA, Steinbrecher KA, Sartor RB, Kohli R, Karp CL, Divanovic S. IL-17 signaling accelerates the progression of nonalcoholic fatty liver disease in mice. *Hepatology.* 2014; 59:1830–1839. [PubMed: 24115079]
 34. Ivanov, Atarashi K, Manel N, Brodie EL, Shima T, Karaoz U, Wei D, Goldfarb KC, Santee CA, Lynch SV, Tanoue T, Imaoka A, Itoh K, Takeda K, Umesaki Y, Honda K, Littman DR. Induction of intestinal Th17 cells by segmented filamentous bacteria. *Cell.* 2009; 139:485–498. [PubMed: 19836068]
 35. Tsai S, Clemente-Casares X, Revelo XS, Winer S, Winer DA. Are obesity-related insulin resistance and type 2 diabetes autoimmune diseases? *Diabetes.* 2015; 64:1886–1897. [PubMed: 25999531]
 36. Wang XA, Zhang R, Zhang S, Deng S, Jiang D, Zhong J, Yang L, Wang T, Hong S, Guo S, She ZG, Zhang XD, Li H. Interferon regulatory factor 7 deficiency prevents diet-induced obesity and insulin resistance. *Am J Physiol Endocrinol Metab.* 2013; 305:E485–495. [PubMed: 23695216]
 37. Sharifnia T, Antoun J, Verriere TG, Suarez G, Wattacheril J, Wilson KT, Peek RM Jr, Abumrad NN, Flynn CR. Hepatic TLR4 signaling in obese NAFLD. *Am J Physiol Gastrointest Liver Physiol.* 2015; 309:G270–278. [PubMed: 26113297]
 38. Wang XA, Zhang R, Jiang D, Deng W, Zhang S, Deng S, Zhong J, Wang T, Zhu LH, Yang L, Hong S, Guo S, Chen K, Zhang XF, She Z, Chen Y, Yang Q, Zhang XD, Li H. Interferon regulatory factor 9 protects against hepatic insulin resistance and steatosis in male mice. *Hepatology.* 2013; 58:603–616. [PubMed: 23471885]
 39. Wang XA, Zhang R, She ZG, Zhang XF, Jiang DS, Wang T, Gao L, Deng W, Zhang SM, Zhu LH, Guo S, Chen K, Zhang XD, Liu DP, Li H. Interferon regulatory factor 3 constrains IKKbeta/NF-kappaB signaling to alleviate hepatic steatosis and insulin resistance. *Hepatology.* 2014; 59:870–885. [PubMed: 24123166]
 40. Wieser V, Adolph TE, Grander C, Grabherr F, Enrich B, Moser P, Moschen AR, Kaser S, Tilg H. Adipose type I interferon signalling protects against metabolic dysfunction. *Gut.* 2016
 41. Franceschini L, Realdon S, Marcolongo M, Mirandola S, Bortoletto G, Alberti A. Reciprocal interference between insulin and interferon-alpha signaling in hepatic cells: a vicious circle of clinical significance? *Hepatology.* 2011; 54:484–494. [PubMed: 21538438]
 42. Bhattacharya A, Hegazy AN, Deigendesch N, Kosack L, Cupovic J, Kandasamy RK, Hildebrandt A, Merkler D, Kuhl AA, Vilagos B, Schliehe C, Panse I, Khamina K, Baazim H, Arnold I, Flatz L, Xu HC, Lang PA, Aderem A, Takaoka A, Superti-Furga G, Colinge J, Ludewig B, Lohning M, Bergthaler A. Superoxide Dismutase 1 Protects Hepatocytes from Type I Interferon-Driven Oxidative Damage. *Immunity.* 2015; 43:974–986. [PubMed: 26588782]
 43. York AG, Williams KJ, Argus JP, Zhou QD, Brar G, Vergnes L, Gray EE, Zhen A, Wu NC, Yamada DH, Cunningham CR, Tarling EJ, Wilks MQ, Casero D, Gray DH, Yu AK, Wang ES, Brooks DG, Sun R, Kitchen SG, Wu TT, Reue K, Stetson DB, Bensinger SJ. Limiting Cholesterol Biosynthetic Flux Spontaneously Engages Type I IFN Signaling. *Cell.* 2015; 163:1716–1729. [PubMed: 26686653]
 44. Barbalat R, Ewald SE, Mouchess ML, Barton GM. Nucleic acid recognition by the innate immune system. *Annual review of immunology.* 2011; 29:185–214.
 45. Miele L, Valenza V, La Torre G, Montalto M, Cammarota G, Ricci R, Masciana R, Forgione A, Gabrieli ML, Perotti G, Vecchio FM, Rapaccini G, Gasbarrini G, Day CP, Grieco A. Increased intestinal permeability and tight junction alterations in nonalcoholic fatty liver disease. *Hepatology.* 2009; 49:1877–1887. [PubMed: 19291785]
 46. Schneider KM, Bieggs V, Heymann F, Hu W, Dreymueller D, Liao L, Frissen M, Ludwig A, Gassler N, Pabst O, Latz E, Sellge G, Penders J, Tacke F, Trautwein C. CX3CR1 is a gatekeeper for intestinal barrier integrity in mice: Limiting steatohepatitis by maintaining intestinal homeostasis. *Hepatology.* 2015; 62:1405–1416. [PubMed: 26178698]

47. Garcia-Martinez I, Santoro N, Chen Y, Hoque R, Ouyang X, Caprio S, Shlomchik MJ, Coffman RL, Candia A, Mehal WZ. Hepatocyte mitochondrial DNA drives nonalcoholic steatohepatitis by activation of TLR9. *The Journal of clinical investigation*. 2016; 126:859–864. [PubMed: 26808498]
48. Revelo XS, Ghazarian M, Chng MH, Luck H, Kim JH, Zeng K, Shi SY, Tsai S, Lei H, Kenkel J, Liu CL, Tangsombatvisit S, Tsui H, Sima C, Xiao C, Shen L, Li X, Jin T, Lewis GF, Woo M, Utz PJ, Glogauer M, Engleman E, Winer S, Winer DA. Nucleic Acid-Targeting Pathways Promote Inflammation in Obesity-Related Insulin Resistance. *Cell reports*. 2016; 16:717–730. [PubMed: 27373163]
49. Guo B, Chang EY, Cheng G. The type I IFN induction pathway constrains Th17-mediated autoimmune inflammation in mice. *The Journal of clinical investigation*. 2008; 118:1680–1690. [PubMed: 18382764]
50. Wilson EB, Yamada DH, Elsaesser H, Herskovitz J, Deng J, Cheng G, Aronow BJ, Karp CL, Brooks DG. Blockade of chronic type I interferon signaling to control persistent LCMV infection. *Science (New York, NY)*. 2013; 340:202–207.
51. Kumari M, Wang X, Lantier L, Lyubetskaya A, Eguchi J, Kang S, Tenen D, Roh HC, Kong X, Kazak L, Ahmad R, Rosen ED. IRF3 promotes adipose inflammation and insulin resistance and represses browning. *The Journal of clinical investigation*. 2016
52. Ghosh AR, Bhattacharya R, Bhattacharya S, Nargis T, Rahaman O, Duttagupta P, Raychaudhuri D, Liu CS, Roy S, Ghosh P, Khanna S, Chaudhuri T, Tania O, Haak S, Bandyopadhyay S, Mukhopadhyay S, Chakrabarti P, Ganguly D. Adipose Recruitment and Activation of Plasmacytoid Dendritic Cells Fuel Metaflammation. *Diabetes*. 2016; 65:3440–3452. [PubMed: 27561727]
53. Ivashkiv LB, Donlin LT. Regulation of type I interferon responses. *Nat Rev Immunol*. 2014; 14:36–49. [PubMed: 24362405]
54. Crouse J, Kalinke U, Oxenius A. Regulation of antiviral T cell responses by type I interferons. *Nat Rev Immunol*. 2015; 15:231–242. [PubMed: 25790790]
55. Forster S. Interferon signatures in immune disorders and disease. *Immunol Cell Biol*. 2012; 90:520–527. [PubMed: 22491066]
56. Liehl P, Zuzarte-Luis V, Chan J, Zillinger T, Baptista F, Carapau D, Konert M, Hanson KK, Carret C, Lassnig C, Muller M, Kalinke U, Saeed M, Chora AF, Golenbock DT, Strobl B, Prudencio M, Coelho LP, Kappe SH, Superti-Furga G, Pichlmair A, Vigario AM, Rice CM, Fitzgerald KA, Barchet W, Mota MM. Host-cell sensors for Plasmodium activate innate immunity against liver-stage infection. *Nature medicine*. 2014; 20:47–53.
57. Revelo XS, Tsai S, Lei H, Luck H, Ghazarian M, Tsui H, Shi SY, Schroer S, Luk CT, Lin GH, Mak TW, Woo M, Winer S, Winer DA. Perforin is a novel immune regulator of obesity-related insulin resistance. *Diabetes*. 2015; 64:90–103. [PubMed: 25048196]
58. Zhang W, Sargis RM, Volden PA, Carmean CM, Sun XJ, Brady MJ. PCB 126 and other dioxin-like PCBs specifically suppress hepatic PEPCK expression via the aryl hydrocarbon receptor. *PLoS One*. 2012; 7:e37103. [PubMed: 22615911]
59. Jo J, Tan AT, Ussher JE, Sandalova E, Tang XZ, Tan-Garcia A, To N, Hong M, Chia A, Gill US, Kennedy PT, Tan KC, Lee KH, De Libero G, Gehring AJ, Willberg CB, Klenerman P, Bertoletti A. Toll-like receptor 8 agonist and bacteria trigger potent activation of innate immune cells in human liver. *PLoS Pathog*. 2014; 10:e1004210. [PubMed: 24967632]

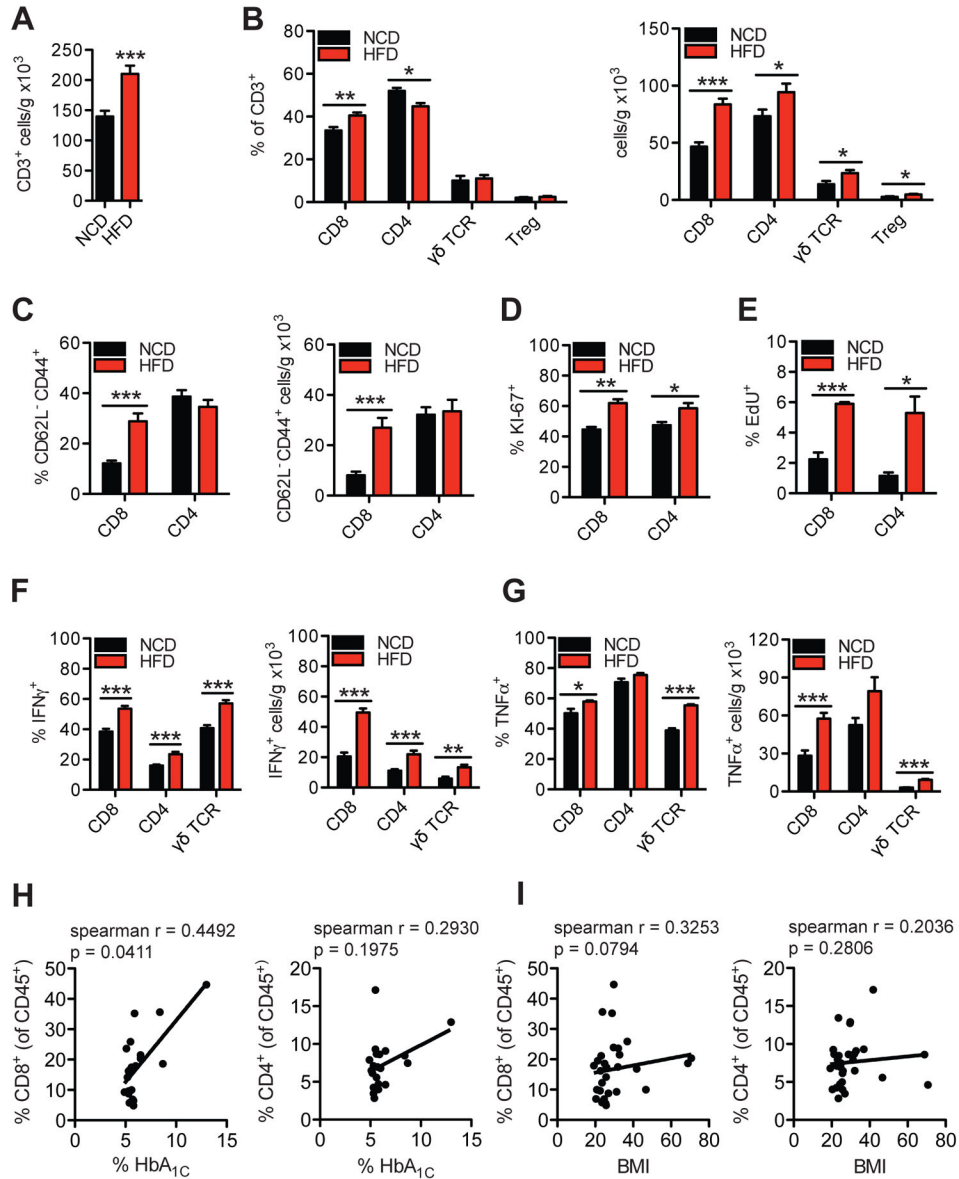


Figure 1. HFD-feeding promotes a pro-inflammatory shift in hepatic T cell populations in mice and hepatic CD8⁺ T cells correlate to glucose dysregulation in humans
 Flow cytometry analysis of liver immune cells isolated from 16 wk HFD- or NCD-fed WT mice representing (A) total number of hepatic CD45⁺CD3⁺NK1.1⁻ gated T cells per gram of tissue (n=16), (B) CD8⁺, CD4⁺, γδTCR⁺, or CD4⁺Foxp3⁺ (Treg) gated hepatic T cell subsets (n=5–16), (C) CD8⁺ or CD4⁺CD62L⁻CD44⁺ gated effector memory T cell subsets (n=15), (D–G) intracellular T cell stains for (D) Ki-67 (n=4), (E) EdU (n=4), (F) IFNγ (n=9), and (G) TNFα (n=4) in CD8⁺, CD4⁺ or γδTCR⁺ gated T cells. Correlative analysis between (H) % CD8⁺ and % HbA_{1c} (left), % CD4⁺ and HbA_{1c} (right), and (I) % CD8⁺ and BMI (left), % CD4⁺ and BMI (right) from human intrahepatic mononuclear cells (HbA_{1c} n=21, BMI n=30). Spearman r values and p values are denoting statistical

significance are indicated in the figure graphs. Statistical significance is denoted by * ($p < 0.05$), ** ($p < 0.01$), and *** ($p < 0.001$).

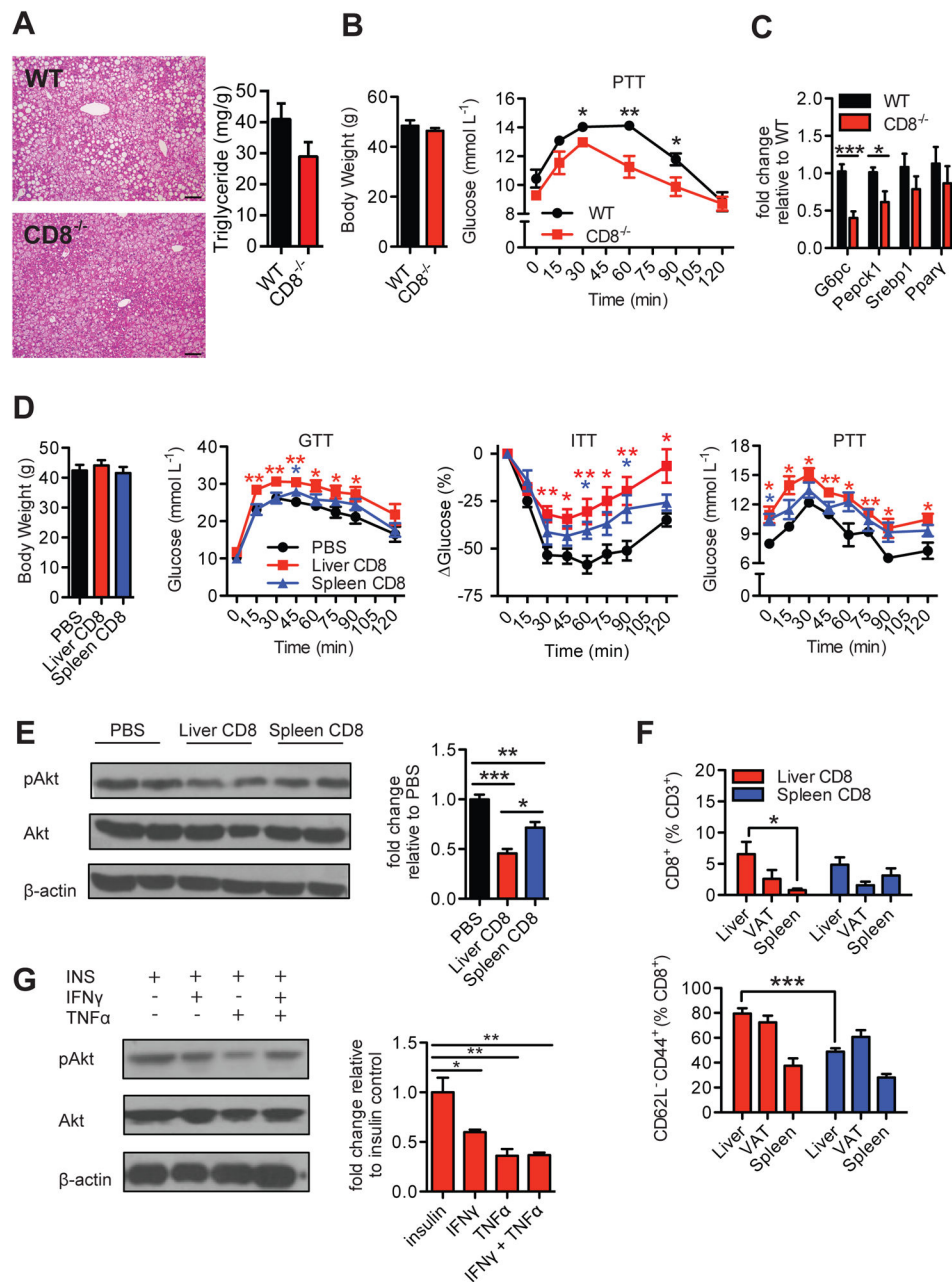


Figure 2. Intrahepatic CD8⁺ T cells drive hepatic insulin resistance

16 wk HFD-fed WT and CD8-deficient (CD8^{-/-}) mice (A) representative H&E liver stains (Left, 200X magnification, Scale bar: 100μm; n=3) and liver triglyceride content (Right, n=5), (B) body weights and pyruvate tolerance test (PTT) (n=5), and (C) RT-PCR gene expression analysis of gluconeogenic enzymes (G6pc, Pepck1) and lipogenic factors (Srebp1, Pparγ) (n=6). (D) Body weights, glucose tolerance test (GTT) (n=6, 2 experiments), insulin tolerance test (ITT) (n=6, 2 experiments), and PTT (n=3) of 16 wk HFD-fed CD8^{-/-} mice 1 week after receiving i.v. transfers of 5×10⁶ negatively sorted intrahepatic or splenic CD8⁺ T cells, or PBS control. Statistical analysis is represented relative to PBS control group. (E) Representative western blot and analysis of liver lysates

immunoblotted for phosphorylated and total Akt proteins after acute insulin injection of transfer mice (n=5), and **(F)** flow cytometry analysis of total CD8⁺ T cell and CD8⁺ effector memory T cells in liver, visceral adipose tissue (VAT), and spleens of transfer mice (n=4–6). **(G)** Representative western blot of pAkt/Akt and analysis of primary hepatocytes treated with 20 ng/ml IFN γ , 20 ng/ml TNF α , or both, or untreated for 24 hrs at 37°C and subsequently treated with 100 nM insulin for 15 min (n=4). Western blot analysis is represented as pAkt/Akt expression relative to control (insulin) group. Statistical significance is denoted by * (p<0.05), ** (p<0.01), and *** (p<0.001).

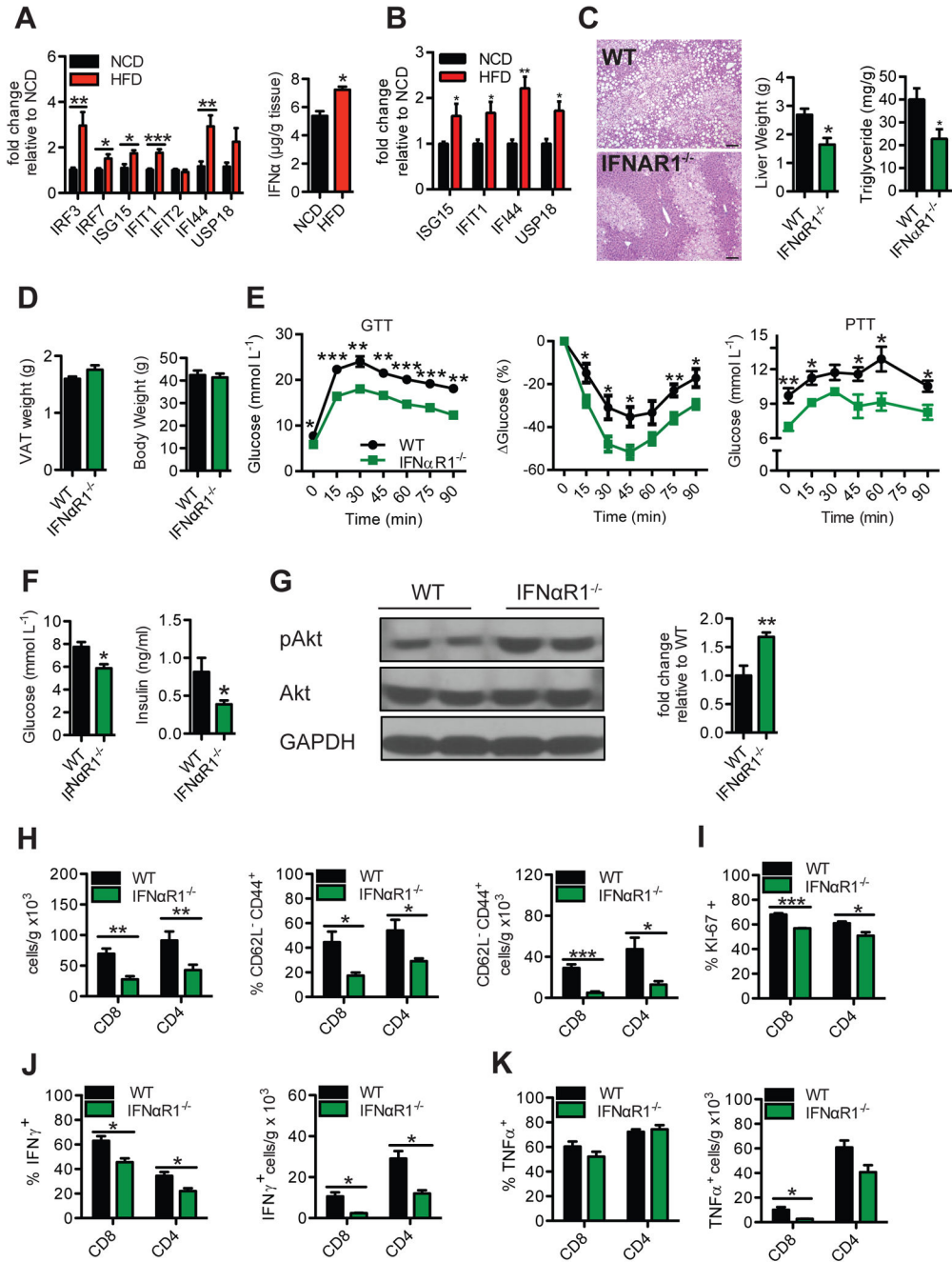


Figure 3. HFD-feeding induces a type I interferon response in the liver that promotes hepatic T cell inflammation and insulin resistance

(A) RT-PCR gene expression analysis of type I interferon (IFN-I) related interferon regulatory factors (IRFs) and interferon stimulatory genes (ISGs) (left, n=8–12), and quantification of IFN α protein (right, n=5) in liver lysates of 16 wk HFD- or NCD-fed WT mice (n=7–10). (B) Gene expression analysis of ISGs in CD8 $^{+}$ T cells from the livers of 16 wk HFD- or NCD-fed WT mice (n=5). (C–K) 16 wk HFD-fed WT and IFN α R1 $^{-/-}$ mice. Representative H&E stain of livers (C, Left; 100X magnification, Scale bar: 100 μ m) (n=3), liver weights (C Middle, n=5), liver triglycerides (C Right, n=5), VAT

weights (**D Left**), body weights (**D Right**), GTT (**E Left**; n=4 for WT, n=5 for KO), ITT (**E Middle**, n=5) and PTT (**E Right**, n=5), fasting glucose (**F Left**, n=4 for WT, n=5 for KO) and insulin (**F Right**, n=8–12), representative western blot and analysis of pAkt/Akt in liver lysates after acute insulin challenge in mice (**G**, n=4–5), flow cytometry analysis of T cell subsets (**H**, n=5), and intracellular T cell staining for (**I**) Ki-67, (**J**) IFN γ and (**K**) TNF α (n=3) using previously stated gating strategies. Western blot analysis is represented as pAkt/Akt expression relative to control group. Statistical significance is denoted by * (p<0.05), ** (p<0.01) and *** (p<0.001).

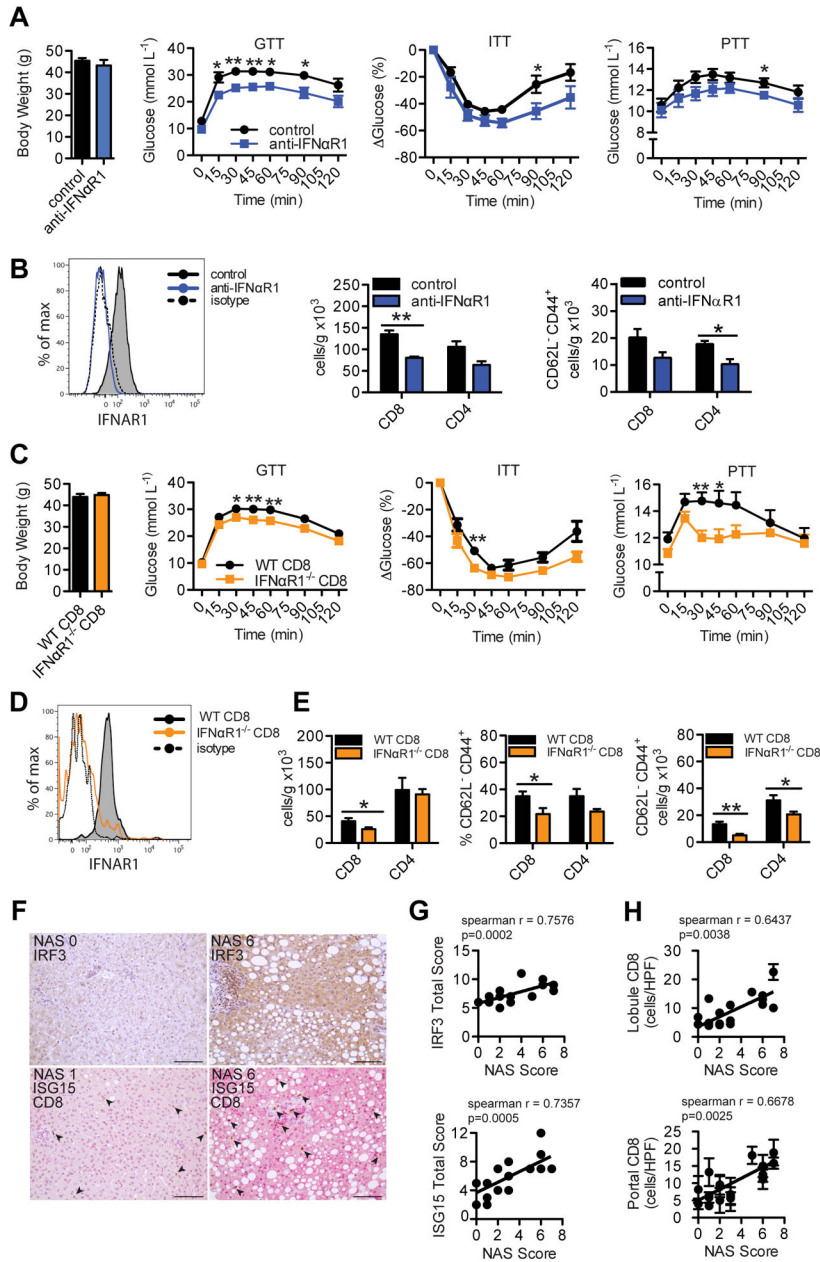


Figure 4. Intrahepatic type I interferon signaling and responsive CD8+ T cells promote metabolic disease in mice and correlate to worsened NAFLD in humans

(A) Body weights, GTT, ITT and PTT (n=5), and (B) flow cytometry analysis of IFNαR1 expression on CD8+ T cells (representative plot) and hepatic T cell subsets (n=3–4) in WT HFD-fed mice that were treated i.p. with 400 μg/wk of anti-IFNαR1 blocking antibody, or IgG control, for 5 wks beginning at 10 wks of HFD-feeding. (C) Body weight (n=10), GTT (n=10), ITT (n=5), PTT (n=10), (D) flow cytometry analysis of IFNαR1 expression on CD8+ T cells (representative plot) and (E) hepatic T cell subsets in 16 wk HFD-fed BM chimeric mice containing (WT CD8) or lacking (IFNαR1^{-/-} CD8) IFNαR1 expression in CD8+ T cells (n=10). T cells were analyzed using previously stated gating strategies. (F)

Representative immunohistochemical staining of human liver biopsies (n=18) given NAS scores and stained single stained for IRF3 (brown), or double stained for ISG15 (pink) and CD8 (brown) (200X magnification, Scale bar: 100 μ m), and correlative analysis between **(G)** NAS Score and IRF3 (top, n=19) or ISG15 (bottom, n=18) protein expression, and **(H)** NAS Score and lobular (top) or portal tract (bottom) CD8+ cells/high power field (HPF = 0.237 mm²) (n=18). Arrows indicate CD8+ cells. Spearman r values and p values denoting statistical significance are indicated in the figure graphs. Statistical significance is denoted by * (p<0.05), and ** (p<0.01).